



**HAL**  
open science

# The role of spin-orbit coupling in the optical spectroscopy of atomic sodium isolated in solid xenon

P. de Pujo, M. Ryan, C. Crépin, J.-M. Mestdagh, J. Mccaffrey

## ► To cite this version:

P. de Pujo, M. Ryan, C. Crépin, J.-M. Mestdagh, J. Mccaffrey. The role of spin-orbit coupling in the optical spectroscopy of atomic sodium isolated in solid xenon. *Low Temperature Physics*, 2019, 45 (7), pp.715-720. 10.1063/1.5111294 . hal-02329620

**HAL Id: hal-02329620**

**<https://hal.science/hal-02329620>**

Submitted on 21 Sep 2020

**HAL** is a multi-disciplinary open access archive for the deposit and dissemination of scientific research documents, whether they are published or not. The documents may come from teaching and research institutions in France or abroad, or from public or private research centers.

L'archive ouverte pluridisciplinaire **HAL**, est destinée au dépôt et à la diffusion de documents scientifiques de niveau recherche, publiés ou non, émanant des établissements d'enseignement et de recherche français ou étrangers, des laboratoires publics ou privés.

# The role of spin-orbit coupling in the optical spectroscopy of atomic sodium isolated in solid xenon

Cite as: Low Temp. Phys. **45**, 715 (2019); <https://doi.org/10.1063/1.5111294>

Published Online: 23 July 2019

P. de Pujo, M. Ryan, C. Crépin, J.-M. Mestdagh, and J. G. McCaffrey



View Online



Export Citation



CrossMark

## ARTICLES YOU MAY BE INTERESTED IN

[Bi<sub>2</sub>Ne: Weakly bound cluster of diatomic bismuth with neon](#)

Low Temperature Physics **45**, 689 (2019); <https://doi.org/10.1063/1.5111288>

[Electron-induced delayed desorption of solid argon doped with methane](#)

Low Temperature Physics **45**, 721 (2019); <https://doi.org/10.1063/1.5111295>

[Triplet emission of atomic ytterbium isolated in a xenon matrix](#)

Low Temperature Physics **45**, 707 (2019); <https://doi.org/10.1063/1.5111293>

LOW TEMPERATURE TECHNIQUES  
**OPTICAL CAVITY PHYSICS**  
 MITIGATING THERMAL  
 & VIBRATIONAL NOISE

**DOWNLOAD THE WHITE PAPER**

downloads.montanainstruments.com/optical\_cavities

MONTANA INSTRUMENTS  
 COLD SCIENCE MADE SIMPLE



# The role of spin-orbit coupling in the optical spectroscopy of atomic sodium isolated in solid xenon

Cite as: Fiz. Nizk. Temp. **45**, 836–842 (July 2019); doi: [10.1063/1.5111294](https://doi.org/10.1063/1.5111294)  
Submitted: 24 May 2019



P. de Pujo,<sup>1,a)</sup> M. Ryan,<sup>2</sup> C. Crépin,<sup>3</sup> J.-M. Mestdagh,<sup>1</sup> and J. G. McCaffrey<sup>2,b)</sup>

## AFFILIATIONS

<sup>1</sup>Laboratoire Interactions, Dynamiques et Lasers (LIDyL) CEA, CNRS and Université Paris-Saclay—UMR 9222 CEA Saclay F-91191 Gif-sur-Yvette, France

<sup>2</sup>Department of Chemistry, National University of Ireland—Maynooth, Maynooth, County Kildare, Ireland

<sup>3</sup>Institut des Sciences Moléculaires d'Orsay (ISMO), UMR 8214, CNRS, Univ. Paris-Sud, Université Paris-Saclay, F-91405 Orsay Cedex, France

<sup>a)</sup>In memoriam, deceased July 2016.

<sup>b)</sup>E-mail: [John.McCaffrey@mu.ie](mailto:John.McCaffrey@mu.ie)

## ABSTRACT

Molecular dynamics calculations, based on the diatomics-in-molecules method, have been used to probe the manifestations of spin-orbit (SO) coupling in the experimental absorption bands of atomic sodium isolated in solid xenon. Inclusion of SO coupling of  $-320\text{ cm}^{-1}$  in spectral simulations of the  $3p^2P \leftarrow 3s^2S$  transition leads to unequal band spacings which very closely match the asymmetrical bandshape observed for blue single vacancy (SV) site occupancy. This SO value, extracted in a previous MCD study, reveals the dramatic change in the effective SO coupling constant of the Na atom (from the gas phase value of  $+17\text{ cm}^{-1}$ ) in solid Xe when it is close to the 12 xenon atoms in the first surrounding sphere. In contrast, the symmetrical three-fold split band of the red tetra vacancy (TV) site in Na/Xe is not affected nearly as much by SO coupling. This reflects a greatly reduced “external heavy atom” effect when the 24 Xe atoms surrounding the Na atom in TV are located at greater distances. The contrasting behavior of sodium in the SV and TV sites suggests a strong dependence of the SO coupling strength on the Na–Xe distance.

Published under license by AIP Publishing. <https://doi.org/10.1063/1.5111294>

## 1. INTRODUCTION

The spectroscopy of alkali atoms isolated in rare gas matrices has attracted attention for more than fifty years.<sup>1,2</sup> Initial motivations were the relatively simple spectroscopy of the alkali atoms and the hope for a detailed theoretical understanding of the experimental observations. Absorption and emission spectra of sodium embedded in rare gas solids were reported in several works with sodium atoms generated by different techniques.<sup>3–5</sup> The observed spectra suggested that the atom was trapped in more than one site. The absorption features of alkali atoms in rare gas matrices exhibit a triplet structure and magnetic circular dichroism (MCD) experiments<sup>4</sup> demonstrated that the dynamical Jahn–Teller effect is responsible for this structure. More recently, molecular dynamics calculations in combination with experiments were conducted to describe an alkali atom (Na) in a matrix environment (Ar and Kr).<sup>6</sup> The focus was on the nature of the trapping sites.

Experiments were also conducted in solid xenon (Xe matrices),<sup>6</sup> revealing the presence of two sites: a stable one (absorption spectrum around 560 nm: the “blue” site) and a thermally unstable one (absorption spectrum around 600 nm: the “red” site). These results were in agreement with previous studies<sup>4,5</sup> in which it was assumed that the stable site arose from single vacancy (SV) occupancy—Na taking the place of one Xe atom in the lattice.<sup>5–7</sup> The triplet structure of the absorption in the blue site exhibits “atypical” splitting between the three components. However, this structure is well explained by a Jahn–Teller effect thanks to the recorded MCD spectra allowing an analysis in terms of coupling with phonon modes.<sup>4</sup> The MCD analysis also revealed a pronounced “heavy atom” effect on the spin-orbit (SO) coupling of the sodium atom isolated in the blue site of xenon.

The theoretical investigations by Gervais’ group in Caen has shown that in alkali (A)–rare gas (RG) pairs, the spin-orbit coupling depends strongly on the alkali–rare gas distance  $R_{A-RG}$ .<sup>8,9</sup>

The effect is especially large when a light alkali atom (e.g., Na) interacts with a heavy rare gas (e.g., Xe). For instance, considering the energy levels, which correlate with the first  $^2P$  state of the alkali atom at infinite  $R_{A-RG}$  separation, the molecular spin-orbit coefficients  $a(R_{Na-Xe}) = \langle ^2\Pi_{1/2} | H_{SO} | ^2\Pi_{1/2} \rangle$  and  $b(R_{Na-Xe}) = \langle ^2\Pi_{-1/2} | H_{SO} | ^2\Sigma_{1/2} \rangle$  of the Na-Xe pair, vary from  $+5.7 \text{ cm}^{-1}$  at infinite Na-Xe separation to  $+27.5$  and  $-21.1 \text{ cm}^{-1}$ , respectively, when  $R_{Na-Xe} = 3.4 \text{ \AA}$ . The latter distance corresponds to the bond length of the deeply bound excited  $A^2\Pi_{1/2}$  state of diatomic Na-Xe.

We anticipate that the “atypical” splitting observed in the recorded Na/Xe spectra is, as mentioned above, due to the occurrence of spin-orbit coupling. This is partly justified by the MCD work of Schatz and coworkers<sup>4</sup> which indicates a strong modification of the spin-orbit coupling in Na when trapped in a xenon matrix. This effect was observed in other metal atom/rare gas samples.<sup>2</sup> The present work aims at exploring the consequences of the spin-orbit coupling on the absorption spectroscopy of atomic sodium isolated in a xenon matrix. The absorption profiles arising from the resonance  $3p^2P \leftarrow 3s^2S$  transition of Na are analysed for both the thermally unstable “red” trapping site band and the stable “blue” site band, present alone in annealed samples.

Preliminary results appeared in Ref. 6, which dealt almost exclusively with the isolation of sodium in argon and krypton matrices. The Na/Xe findings presented here follow the same approach in which the experimental data are compared with spectral simulations emerging from molecular dynamics calculations that utilize a simple numerical approach to generate the solid-state potentials. With this method, the electronic problem is treated by the pair-wise addition of the Na-Xe potentials within the Diatomic-In-Molecule (DIM) formalism.<sup>10-14</sup> Although more refined treatments exist which include many body effects, e.g., the one-electron model based on core polarization pseudo-potentials developed by Gervais’ group,<sup>9,15</sup> the simpler DIM approach is appropriate here for the flexibility it provides to turn on and off the effect of spin-orbit coupling in the spectral simulations.

## 2. EXPERIMENTAL

### 2.1. Experimental setup

The experimental apparatus used in the preparation of Na/Xe matrices and the set up used to record spectra have been described in previous publications from the Maynooth group.<sup>16</sup> Solid Na/Xe samples were prepared by co-condensing Na vapor, produced by electron bombardment of Na metal in a Mo crucible, with xenon onto a cold  $\text{CaF}_2$  window. Samples were deposited at temperatures ranging from 12 to 35 K. Low temperatures were achieved using an APD cryogenic closed-cycle helium displacer system (HC-2D). The temperature was monitored with a silicon diode sensor placed on the copper holder of the  $\text{CaF}_2$  window. High vacuum ( $10^{-7}$  mbar) within the sample chamber was maintained by an Edwards oil vapor diffusion pump (EO2K) backed with an Edwards rotary vacuum pump (E2M2) and monitored by an Alcatel CF2P Penning gauge.

Vacuum in the gas-handling system (GHS), on the order of  $10^{-8}$  mbar, was monitored by an ionization gauge and maintained by a Balzers-Pfeiffer turbo-molecular pump (TPU-180H).

Two Tylan General baratron capacitance manometers were used to monitor the amounts of gas in the GHS. A Granville-Phillips (GP model 203) variable leak valve controlled the gas flow rate onto the cold  $\text{CaF}_2$  window, the rate generally being between 3.8 and 4.8  $\text{mmol h}^{-1}$ . The output of a continuous tungsten lamp, dispersed with a 0.3 m Acton Research Corporation SpectraPro SP-300i (ARC SP-300i) monochromator, was used to excite Na within the Xe matrix. Transmittance spectra were obtained with a Hamamatsu IP28 photomultiplier tube (PMT) by scanning the ARC SP-300i.

### 2.2. Experimental results

The absorption spectrum recorded in the region of the  $3p^2P \leftarrow 3s^2S$  transition of atomic sodium deposited in a solid xenon matrix at 12.7 K is shown in the top panel of Fig. 1.

The well-known yellow emission of atomic Na in the gas-phase consists of a pair of lines at 16956.17 and 16973.36  $\text{cm}^{-1}$  whose splitting of 17.2  $\text{cm}^{-1}$  arises from the weak spin-orbit coupling constant of this light metal atom. The location of the former line is indicated by the vertical line in Fig. 1 near 589.7 nm. In solid xenon, a pair of bands, each with a threefold splitting, dominate the freshly deposited spectrum as shown in the top panel.

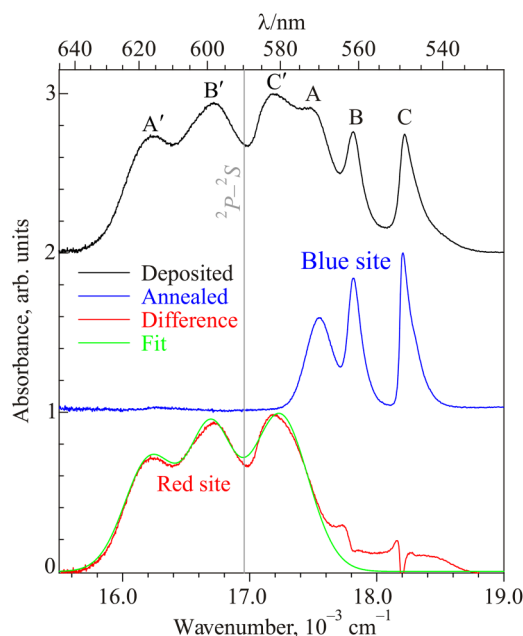


**FIG. 1.** Absorption spectra recorded at  $T = 12.7 \text{ K}$  for atomic Na isolated in a solid xenon matrix. The top panel shows the spectrum on deposition while that in the middle presents the blue site bands recorded after annealing the matrix to 35 K. In the bottom panel the red site spectrum, obtained as the difference of the freshly deposited and annealed scans, is shown by the red curve. As is evident by the complex structure in the blue portion of the difference spectrum, lineshape changes of the blue site occur on annealing. To obtain the isolated red site profile the results of a fit, done with three Gaussian curves is shown by the green trace. The vertical line indicates the position of the atomic Na  $3p^2P \leftarrow 3s^2S$  transition in the gas phase.

The existence of this pair of bands suggests that two trapping sites are present, namely the red site ( $A'$ ,  $B'$  and  $C$  features) and the blue site ( $A$ ,  $B$  and  $C$  features). This anticipation is confirmed upon annealing the matrix up to 35 K as shown in the middle panel of Fig. 1. Only the three higher energy peaks pertaining to the blue site remain. This band is located entirely on the blue side of the gas phase Na resonance  $3p^2P \leftarrow 3s^2S$  transition and its shape is remarkable. From red to blue, the features centered at 17,553 and 17,816  $\text{cm}^{-1}$  are separated by only 263  $\text{cm}^{-1}$  whereas the feature at 18,211  $\text{cm}^{-1}$  is more distant, separated by 395  $\text{cm}^{-1}$  from the middle feature. The width of the blue peak is also noteworthy as it is considerably narrower than the typical absorption profiles of matrix-isolated metal atoms.<sup>2</sup>

In contrast, the red site is found to disappear completely from the matrix at approximately 30 K and is clearly thermally unstable. Such behavior has been observed in earlier works.<sup>4,5</sup> The location and bandshape of the red site is presented in the bottom panel of Fig. 1. It was obtained in the present study as the difference spectrum of the freshly deposited and annealed scans and is shown by the red trace. As is evident by the complex structure in the blue portion of the difference spectrum, lineshape changes of the blue site occur on annealing. To obtain the isolated red site profile, the results of a fit, done with three Gaussian curves is shown by the green trace. The parameters of the fit involved three bands centered at 16220, 16694 and 17235  $\text{cm}^{-1}$  with (fwhm) widths of 477, 404 and 522  $\text{cm}^{-1}$ , respectively. The symmetric shape of the resulting profile is typical of spectra recorded for  $P \leftarrow S$  transitions of metal atoms isolated in the solid rare gases.

### 3. SIMULATION OF THE ABSORPTION SPECTRUM

#### 3.1. Simulation technique

Simulation of the absorption spectrum was performed using the same method as that reported in Ref. 6. Atomic Na isolated in the Xe matrix was modeled as a  $\text{NaXe}_n$  cluster and followed the strategy developed by Visticot *et al.*<sup>17</sup> An alternative strategy could have been Monte-Carlo simulations, such as those done by Lawrence and Apkarian, rather than the Molecular Dynamics calculations conducted in the present work.<sup>18</sup> Molecular dynamics were also conducted to simulate the formation of the matrix itself in order to characterize the most stable sites. The method to simulate sample deposition and thereby obtain the stable sites is described in Ref. 6.

The simulation of the spectra is performed in four steps: i) construction of a  $\text{Na}(\text{Xe})_{1291}$  cluster to mimic Na in the matrix environment; ii) generating the Hamiltonians describing both ground and excited  $\text{Na}(\text{Xe})_{1291}$  from additive pair potentials within the Diatomics-in-Molecule (DIM) formalism; iii) following the classical evolution of the system in the ground state by a Molecular Dynamics (MD) calculation, whereby the distribution of nuclear configurations of the atoms on the ground state potential energy surface is established; iv) adding the excited electronic energies of each Na–Xe pair in the total Hamiltonian describing each configuration. Diagonalisation follows and three transition energies are obtained. A histogram of these energies is built when sampling all the configurations stored at step iii). This energy summation generates the simulated absorption spectrum. Details of steps i)–iii) are given below.

*Step i)* A cluster of 1292 xenon atoms is built first. It consists of nine layers of an *fcc* crystal with a lattice parameter of 6.13 Å. Following our previous work on sodium trapped in argon and krypton matrices,<sup>6</sup> two trapping sites are considered, a single vacancy site (SV) and a tetra vacancy site (TV) (see Sec. 4). A Xe atom at the center of the cluster is replaced by a sodium atom to mimic a substitution trapping (SV) site of the matrix. The resulting  $\text{Na}(\text{Xe})_{1291}$  cluster is used as the initial geometry for the molecular dynamics calculations. For the TV site, four adjacent Xe atoms surrounding a tetrahedral interstitial site are removed and replaced by a single Na atom. MD calculations were then run for the resulting  $\text{Na}(\text{Xe})_{1288}$  cluster.

*Step ii)* The pair potentials which are included in the Di-atomics-in-Molecule (DIM) formalism describe the Xe–Xe and Na–Xe interactions. For Xe–Xe, only the ground electronic state needs to be considered. A simple Lennard-Jones (12–6) function was used. It is parametrized with  $\epsilon = 191.3 \text{ cm}^{-1}$  and  $\sigma = 3.88 \text{ Å}$ .<sup>19</sup> For Na–Xe, both the ground state and the excited electronic states correlating to  $\text{Na}(3p^2P) + \text{Xe}$  at infinite separation need to be considered. Their inclusion into the DIM formalism is different depending on whether the spin-orbit interaction is included or not.

When not including the spin-orbit interaction, three potential energy curves  $X^2\Sigma$ ,  $A^2\Pi$  and  $B^2\Sigma$  describe the Na–Xe interaction. They are documented in an extensive investigation of the electronic state properties of the Na–Xe pair using *ab initio* methodologies and various pseudopotential approaches.<sup>20</sup> The latter work includes a reference calculation for the low lying states  $X^2\Sigma$ ,  $A^2\Pi$  and  $B^2\Sigma$ . For its use in the present DIM calculations, the  $X^2\Sigma$  potential curve was fit with the expression

$$V(R_{\text{Na-Xe}}) = \sum_i \frac{C_{\{2i\}}}{R_{\text{Na-Xe}}^{2i}}. \quad (1)$$

The resulting fit parameters where  $i$  varies from 3 to 7 are given in Table I. Similar expressions where  $i$  varies up to  $i = 12$  are used to fit the  $A^2\Pi$  and  $B^2\Sigma$  potential energy curves. They have no particular physical meaning, beyond being fit parameters. Their values are reported in Table I.

**TABLE I.** Parameters used in Eq. (1) to fit the  $X^2\Sigma$ ,  $A^2\Pi$  and  $B^2\Sigma$  potential energy curves provided in Ref. 20 for the Na–Xe interaction.

$C_n, \text{ cm}^{-1} \text{ Å}^n$	$X^2\Sigma$	$A^2\Pi$	$B^2\Sigma$
$C_6$	$-8.430 \ 4 \cdot 10^6$	$-7.604 \ 3 \cdot 10^6$	$5.775 \ 4 \cdot 10^6$
$C_8$	$2.153 \ 5 \cdot 10^8$	$1.077 \ 3 \cdot 10^8$	$-5.603 \ 3 \cdot 10^9$
$C_{10}$	$-1.841 \ 9 \cdot 10^9$	$-4.367 \ 2 \cdot 10^8$	$4.876 \ 3 \cdot 10^{11}$
$C_{12}$	$7.515 \ 0 \cdot 10^9$	$8.178 \ 6 \cdot 10^8$	$-1.871 \ 5 \cdot 10^{13}$
$C_{14}$	$-1.156 \ 1 \cdot 10^{10}$	$-6.767 \ 0 \cdot 10^8$	$4.101 \ 5 \cdot 10^{14}$
$C_{16}$		$1.455 \ 3 \cdot 10^8$	$-5.600 \ 4 \cdot 10^{15}$
$C_{18}$			$4.862 \ 8 \cdot 10^{16}$
$C_{20}$			$-2.613 \ 0 \cdot 10^{17}$
$C_{22}$			$7.915 \ 7 \cdot 10^{17}$
$C_{24}$			$-1.031 \ 3 \cdot 10^{18}$

The three NaXe potentials used in the present work are shown in Fig. 2 where they are compared with the ground state potential of Xe<sub>2</sub>. This comparison reveals how well matched the ground states of NaXe ( $X^2\Sigma$ ) (blue trace) and Xe<sub>2</sub> (black trace) are, particularly at their energy minima. A consequence of which is the favourable isolation of sodium in a single vacancy site in solid xenon. The energetics of diatomic NaXe at the SV and TV site sizes are also provided in Fig. 2. It is evident there that the latter site is de-stabilised by approximately 31 cm<sup>-1</sup> relative to the SV site. This may be the reason for the thermal instability of the larger TV site as observed in the annealing study.

When including spin-orbit coupling, four potential energy curves  $X^2\Sigma_{1/2}$ ,  $A^2\Pi_{1/2}$ ,  $A^2\Pi_{3/2}$  and  $B^2\Sigma_{1/2}$  are required to describe the Na–Xe interaction. They are easy to deduce from the  $X^2\Sigma$ ,  $A^2\Pi$ , and  $B^2\Sigma$  curves when the spin-orbit coupling does not depend on the internuclear distance,  $R_{\text{Na-Xe}}$ . The formalism which allows determining the interaction Hamiltonian plus the spin-orbit Hamiltonian in the coupled  $|(\ell s)j, m_j\rangle$  basis set is fully described by Lawrence and Apkarian.<sup>18</sup> It is used here assuming that the spin-orbit coupling ( $\Delta$  in the notation of Lawrence and Apkarian) is equal to  $-320$  cm<sup>-1</sup>, the value obtained from MCD experiments in Na/Xe.<sup>4</sup>

*Step iii)* The MD calculation was run for 10 ns in steps of 5 fs. The first 5 ns served to stabilize the Na(Xe)<sub>1291</sub> and Na(Xe)<sub>1288</sub> clusters at the working temperature  $T$  for the SV and TV sites, respectively. We consider that full thermalization was achieved since the average potential energy no longer varied significantly after 5 ns. A geometry was saved every 500 fs during the remaining

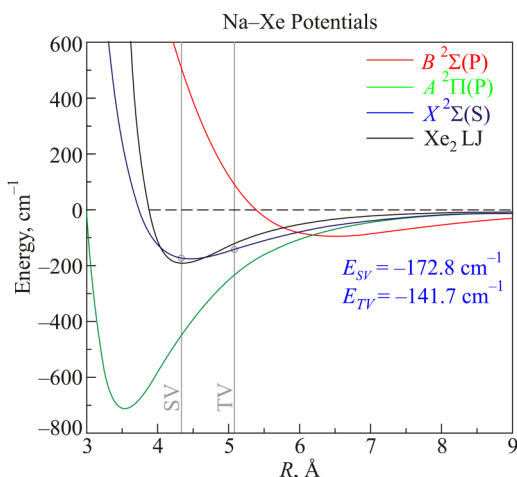


**FIG. 2.** The potential energy curves for the ground  $X$  and excited  $A$  and  $B$  states of NaXe used in the spectral simulations of Na/Xe matrices. The origin of the curves are the *ab initio* calculations of Ref. 20 which are fitted to get the potentials shown. For the purposes of comparison the interaction potential of xenon dimer is also presented. A Lennard-Jones function, with the parameters  $\epsilon = 191.3$  cm<sup>-1</sup> and  $\sigma = 3.88$  Å, was used for Xe<sub>2</sub>. Shown by the vertical lines are the sizes of the single vacancy (SV) and tetra-vacancy (TV) sites in solid xenon. This comparison reveals how well the SV site size and the NaXe  $X$  state bond lengths match and the extent to which the TV site is too large.

5 ns of the MD. This provided us with an extensive body of 10000 configurations. In order to account for the actual motional amplitudes of the atoms in the lattice at the experimental temperature (12.7 K), the MD calculations were conducted at an “effective” temperature  $T$ . At these elevated temperatures it is expected that quantum effects arising from zero point vibrational energy will be accounted for. Different effective temperatures have been suggested following distinct methods developed by several authors.<sup>21–23</sup> These lead to effective temperatures either around 30 K or around 50 K when adapted to the present case. MD calculations were performed at both of these two values to look at the temperature dependence. In fact, a strong temperature dependence was experimentally observed in the spectra of the blue site.<sup>4</sup> As will be shown ahead, the simulated spectra we obtained show that the temperature of 50 K reproduces the present experimental data better. Consequently, the results presented in the following sections were obtained using the higher effective temperature.

### 3.2. Simulation of the deposition

The results of approximately ninety deposition simulations in the Na/Xe system demonstrate that atomic Na prefers to occupy a SV site in the *fcc* lattice. This behavior is consistent with the similarity of the Na-Xe ground state bond length and the SV size of the host matrix (see Fig. 2).

From the experimental work, we know that two sites are formed on deposition, one of which is thermally unstable. Identification therefore, of the second site meant relying on results obtained using the modelling techniques described earlier. In an attempt to reproduce the second site, the conditions of the deposition were varied extensively, in particular the temperature, velocity of the ad-atoms and the relaxation time between the incoming atoms. However, the

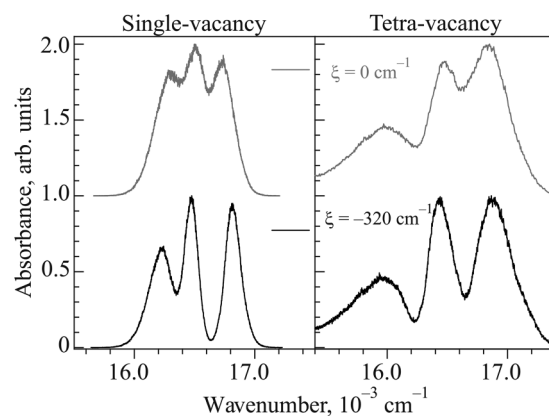


**FIG. 3.** Simulated spectra generated at  $T = 50$  K when neglecting (top traces) and including (bottom traces) the spin-orbit Hamiltonian into the description of the interaction between atomic sodium and the surrounding xenon atoms. The panel on the left shows the results for the SV site of Na/Xe—that on the right shows the results for the TV site. The magnitude of the spin-orbit coupling used was  $-320$  cm<sup>-1</sup> which is the value determined in the matrix MCD study of Na/Xe presented in Ref. 4.

second site has not been observed in simulated depositions. We thereby conclude that the stable site is likely to be a SV site.

### 3.3. Spectral simulations

Figure 3 shows the simulated spectra both with (bottom panel) and without (top panel) the spin-orbit Hamiltonian when describing the interaction between Na and the surrounding Xe atoms in SV and TV sites. Inclusion of spin-orbit coupling has an effect on both simulated spectra but it is especially dramatic for the SV site. Its presence causes the SV spectrum to switch from a regularly spaced threefold splitting—typical of most Jahn–Teller coupled systems—to a situation where the blue feature is significantly more distant from the middle feature than the red one. This effect is less in the TV site but here also there is significant narrowing of the bands. From a comparison of the simulated SV site spectrum and the absorption profile shown in Fig. 1 for the thermally stable site, it is immediately evident that inclusion of the spin-orbit coupling generates the recorded band shape very successfully.

### 4. DISCUSSION AND CONCLUSION

The identities of the sites responsible for the red and blue absorption bands in Na/Xe have been investigated already in frequency shift  $\nu_{\text{abs}}(\text{cm}^{-1})$  versus polarisability plots in Ar, Kr and Xe. From these plots (see Fig. 6 in Ref. 6) and the results of the MD calculations done on the Na/Ar and Na/Kr matrix systems, it is proposed that the two sites are SV and TV sites. The thermally stable blue band arises from a single vacancy (SV) site in agreement with the conclusion from the present simulations of the deposition. The unstable red site is thus attributed to a tetra-vacancy (TV) site. Figure 4, which compares the recorded and simulated spectra was generated in accordance with these site attributions.

Symmetrical three-fold splitting is characteristic of the absorption spectra for  $P \leftarrow S$  transitions of matrix-isolated metal atoms and has been ascribed to the dynamic Jahn–Teller (JT).<sup>4</sup> It arises from coupling between the excited  $P$  state metal atom with the host lattice inducing a temporary break down in the triply degenerate  $P$  energy level. This behavior is related to the site symmetry and such splittings are anticipated in the cases of site occupancy with octahedral or cubo-octahedral symmetry. Simulations of the dynamical JT typically leads to regularly spaced features, as seen for the SV site with no SO included. Regardless of the potential used, the symmetrical three-fold shape remains—only the spacing and width changes.

As is evident in the experimental spectra shown in Fig. 1, symmetrical three-fold splitting is not exhibited by the blue site band recorded for the  $3p^2P \leftarrow 3s^2S$  transition of Na in solid xenon. Inclusion of SO leads, as shown in Fig. 4 to an unequal spacing in the simulated spectrum that matches the recorded bandshape particularly well for the SV site. The value of  $-320 \text{ cm}^{-1}$  reflects the dramatic change of the SO coupling value when the Na atom is close to the 12 Xe atoms in the first surrounding sphere. The fact that our formalism assumes the SO coupling is constant as  $R_{\text{Na-Xe}}$  is varied, is a first approximation, but evidently works well with the SV site. The influence on the Na guest atom is dominated by the first surrounding Xe layer where the SO coupling value used in the calculation simply represents an average value for these nearest

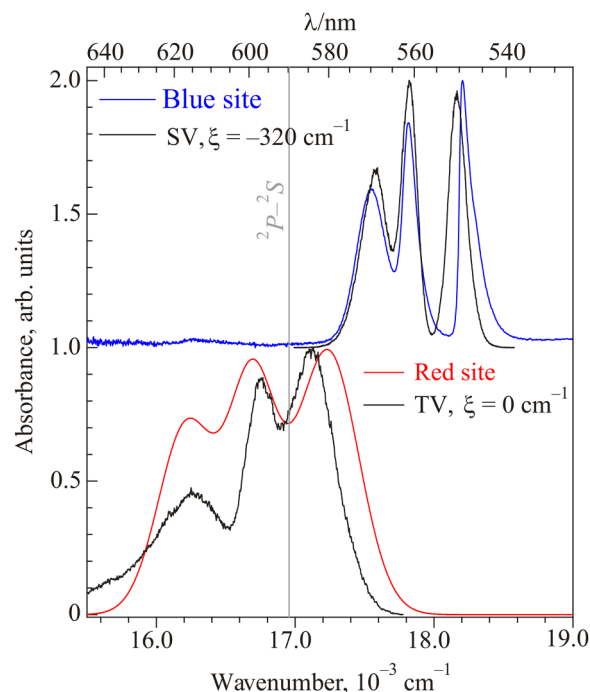


**FIG. 4.** A comparison of the experimental absorption spectra—colour coded for the red and blue sites—with the band shapes simulated (black traces) for the SV and TV sites of Na/Xe. The experimental blue site band was recorded after annealing, while the red site was obtained as a difference spectrum of the freshly deposited and annealed scans. The band shown for the red site is the fit done on the difference spectrum with three Gaussian curves and presented in Fig. 1. In making this comparison with experiment, the simulated bands were generated at an effective temperature of 50 K as outlined in the Methods section. The SV and TV bands have been blue shifted by  $1350$  and  $280 \text{ cm}^{-1}$  respectively to match the observed bands. As indicated, the value of the spin-orbit coupling used for the SV site was  $\zeta = -320 \text{ cm}^{-1}$ , while it was zero for the TV site.

Xe atoms. We performed calculations with SO values ranging between  $0$  and  $-500 \text{ cm}^{-1}$ . The results show a continuous effect on the spacing between the three components and their widths when decreasing this parameter. The “atypical” shape of the triplet structure in absorption is obviously due to the effect of spin-orbit in the cramped site.

Experimentally, the thermally unstable red (TV) site exhibits almost equal spacing of the three bands (gaps of  $475$  and  $540 \text{ cm}^{-1}$ ). This is probably an indication that a smaller SO coupling is at play for this site where the Na–Xe distance is greater than in the SV site. This anticipation fits with the calculations of Gervais *et al.* where the SO coupling is examined as a function of the Na–rare gas distance.<sup>8,9</sup> For this reason, the simulation with no SO is included in Fig. 4 for the TV site.

Beyond the triplet structure, the overall agreement between experiment and simulation is not perfect. In particular, the centre positions of the simulated bands are located to the red of the observed positions for the two sites. As indicated in the caption of

Fig. 4, it is quite small for the TV site but a value of  $1350\text{ cm}^{-1}$  is considerable for the SV site. Moreover, it is also evident that the extension of the simulated spectrum is limited for both sites. These discrepancies are most likely due to the approximations contained in the calculation for the solid-state interaction potential with the DIM method—specifically, the additive use of pair potentials and the accuracy of the Na–Xe potential curves. These limitations have been bypassed in a work of the Gervais group on alkali atoms in an argon matrix where an excellent agreement was found with experiment.<sup>15</sup>

A calculation of this type could be undertaken in the Xe matrix environment. However, the importance of the SO effect that is revealed here, should motivate a full treatment which includes SO coupling.

## REFERENCES

- <sup>1</sup>M. McCarty and G. W. Robinson, *Mol. Phys.* **2**, 415 (1959).
- <sup>2</sup>C. Crépin-Gilbert and A. Tramer, *Int. Rev. Phys. Chem.* **15**, 485 (1999).
- <sup>3</sup>L. C. Balling, M. D. Havey, and J. F. Dawson, *J. Chem. Phys.* **69**, 1670 (1978).
- <sup>4</sup>J. Rose, D. Smith, B. E. Williamson, P. N. Schatz, and M. C. M. O'Brien, *J. Phys. Chem.* **90**, 2608 (1986).
- <sup>5</sup>S. Tam and M. E. Fajardo, *J. Chem. Phys.* **99**, 854 (1993).
- <sup>6</sup>M. Ryan, M. Collier, P. de Pujo, C. Crépin, and J. G. McCaffrey, *J. Phys. Chem. A* **114**, 3011 (2010).
- <sup>7</sup>L. C. Balling and J. J. Wright, *J. Chem. Phys.* **81**, 675 (1984).
- <sup>8</sup>E. Galbis, J. Douady, E. Jacquet, E. Giglio, and B. Gervais, *J. Chem. Phys.* **138**, 014314 (2013).
- <sup>9</sup>B. Gervais, D. Zanuttini, and J. Douady, *J. Chem. Phys.* **144**, 194307 (2016).
- <sup>10</sup>E. Steiner, P. R. Certain, and P. J. Kuntz, *J. Chem. Phys.* **59**, 47 (1973).
- <sup>11</sup>P. J. Kuntz, *Atom Molecule Collision Theory*, edited by R. B. Bernstein (Plenum, New York, 1979), p. 79.
- <sup>12</sup>A. B. Tutein and H. R. Mayne, *J. Chem. Phys.* **108**, 308 (1998).
- <sup>13</sup>O. Roncero, J. A. Beswick, N. Halberstadt, and B. Soep, *Dynamics of Polyatomic van der Waals Complexes*, edited by N. Halberstadt and K. Janda (Plenum, New York, 1990), p. 471.
- <sup>14</sup>M.-C. Heitz, L. Teixidor, N. T. Van-Oanh, and F. Spiegelman, *J. Phys. Chem. A* **114**, 3287 (2010).
- <sup>15</sup>E. Jacquet, D. Zanuttini, J. Douady, E. Giglio, and B. Gervais, *J. Chem. Phys.* **135**, 174503 (2011).
- <sup>16</sup>M. A. Collier and J. G. McCaffrey, *J. Chem. Phys.* **119**, 11878 (2003).
- <sup>17</sup>J. P. Visticot, P. de Pujo, J.-M. Mestdagh, A. Lallement, J. Berlande, O. Sublemontier, P. Meynadier, and J. Cuvellier, *J. Chem. Phys.* **100**, 158 (1994).
- <sup>18</sup>W. G. Lawrence and V. A. Apkarian, *J. Chem. Phys.* **101**, 1820 (1994).
- <sup>19</sup>G. C. Maitland, M. Rigby, E. B. Smith, and W. A. Wakeman, *Intermolecular Forces: Their Origin and Determination* (Oxford University Press, New York, 1987).
- <sup>20</sup>F. Ben Salem, M. Ben El Hadj Rhouma, F. Spiegelman, J.-M. Mestdagh, and M. Hochlaf, *J. Chem. Phys.* **137**, 224310 (2012).
- <sup>21</sup>J. P. Bergsma, P. H. Berens, K. R. Wilson, D. R. Fredkin, and E. J. Heller, *J. Phys. Chem.* **88**, 612 (1984).
- <sup>22</sup>A. Ohnishi and J. Randrup, *Phys. Rev. A* **55**, R3315 (1997).
- <sup>23</sup>L. Uranga-Piña, A. Martínez-Mesa, J. Rubayo-Soneira, and G. Rojas-Lorenzo, *Chem. Phys. Lett.* **429**, 450 (2006).

Translated by AIP Author Services